Author/s:
Chen, S;Gad, E;Zhang, L;Lam, N;Xu, S;Lu, G

Title:
Experiments on an ice ball impacting onto a rigid target

Date:
2022-09-01

Citation:
Chen, S., Gad, E., Zhang, L., Lam, N., Xu, S. & Lu, G. (2022). Experiments on an ice ball impacting onto a rigid target. INTERNATIONAL JOURNAL OF IMPACT ENGINEERING, 167, https://doi.org/10.1016/j.ijimpeng.2022.104281.

Persistent Link:
https://hdl.handle.net/11343/304806

Experiments on an ice ball impacting onto a rigid target

Siyu Chen , Emad Gad , Lihai Zhang , Nelson Lam ,
Shanqing Xu , Guoxing Lu

PII: S0734-743X(22)00127-0
DOI: https://doi.org/10.1016/j.ijimpeng.2022.104281
Reference: IE 104281

To appear in: *International Journal of Impact Engineering*

Please cite this article as: Siyu Chen , Emad Gad , Lihai Zhang , Nelson Lam , Shanqing Xu , Guoxing Lu , Experiments on an ice ball impacting onto a rigid target, *International Journal of Impact Engineering* (2022), doi: https://doi.org/10.1016/j.ijimpeng.2022.104281

Experiments on an ice ball impacting onto a rigid target

Siyu Chen[1], Emad Gad[1], Lihai Zhang[2], Nelson Lam[2], Shanqing Xu[1], Guoxing Lu*[1]

Corresponding author E-mail address: glu@swin.edu.au

1. School of Engineering, Swinburne University of Technology, Hawthorn, VIC 3122, Australia.
2. Department of Infrastructure Engineering, The University of Melbourne, Parkville, VIC 3010, Australia.

HIGHLIGHTS

- The ice ball impact onto a rigid target is extensively investigated in experiments
- Empirical relations are proposed to predict the impact response of ice balls
- The relations can accurately predict the experimental results conducted by others
- The impulse in the impact is equal to the input momentum of ice balls

Graphical Abstract

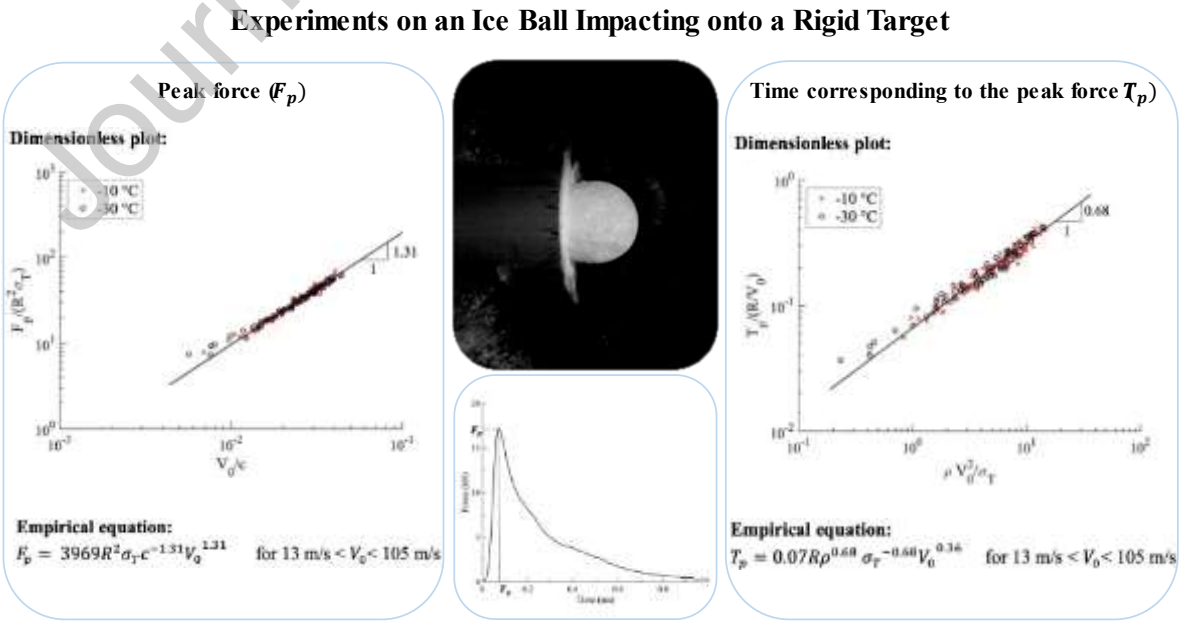

Abstract

This paper is concerned with the peak force (F_p) and time of occurrence (T_p) generated by the spherical ice specimen impacting onto a rigid target. The ice specimens had diameter ranging from 31.8 to 50 mm, and were prepared at temperature of -10 °C and -30 °C, respectively. The key original contribution of the article is the derivation of a correlation relationship for providing accurate predictions of F_p and T_p, for given hail size, velocity and temperature. A total of 149 Hopkinson bar tests were conducted, with impact velocity varying from 13 to 105 m/s for measuring the impact force. The tensile strength of ice, which is a term in the predictive expressions (and is measurable by the Brazilian tests), can be adjusted to take into account changes in temperature of the ice specimen. Experimental results showed that as the size of the ice specimen and its impact velocity increases, F_p increases significantly whereas T_p only increases slightly. Lowering of the temperature resulted in an increase in F_p, and decrease in T_p. Dimensional analysis was employed for processing the experimental data. Empirical relationships expressed as functions of impact velocity, specimen radius, tensile strength of ice, ice density and elastic wave speed of ice were derived. The ratio of the measured impulse to the momentum generated by the impact has also been checked, and was found to be within the range of 0.8 to 1.12. The derived empirical relationships will serve as a guide for further investigations into the structural responses to impact of an ice ball.

Keywords: Ice ball impact, impact force, force-time curve, impulse, dimensional analysis.

1. Introduction

Hailstone impact is one of the most concerned issues among ice impact scenarios of low-to-moderate velocity. As a natural meteorological phenomenon, severe hailstorm may cause disastrous damage to civil infrastructure, assets and agriculture. Damage to cars, roofs

and building claddings accounts for the majority loss in a hailstorm. To mitigate the loss, extensive investigation is needed to understand the severity of damage caused by hailstorms and the related impact response.

The damage severity of a plate subjected to ice impact is one primary concern. Impact of aluminium plates, steel plates and the associated fracture of ice were reported [1-4]. In ice impact, the responses for aluminium plates involve indentation, crack initiation and crack propagation [1]. Strain gauges were attached on the plate surfaces to obtain the strain signals versus time. Various impactors were used [1], including ice cylinders, ice cylinders with a conical tip, and water packed in rubber envelopes. The residual strain after the impact indicated that the cylindrical ice impactor caused much more severe damage to aluminium plates compared with the other two types of impactors, whereas water impactor only led to global bending.

The impact response for composite panels is relatively complex, in which the main failure mechanisms included delamination, fibre failure, cracks and transverse damage [5-11]. For low-velocity impact, delamination occurred first in the panel. With the increase of velocity, fibre failure and cracks were observed. Under very high velocity impact, the panel was perforated. Rhymer et al. [5] characterised the damage resistance of carbon/epoxy composite tape laminates subjected to high velocity ice impact by identifying the threshold energy of failure when delamination occurred. Their study found that the failure threshold energy exhibited a linear relationship to the ratio of panel thickness to ice ball diameter.

The severity of panel damage in ice impact is governed by the force history generated between the impactor and the target. However, direct measurement of the force is challenging. Several studies have been conducted to experimentally extract the force history experienced by a panel under ice impact. Hammetter et al. [12] used the Sum of Weighted Accelerations Technique (SWAT) to measure the impulse produced by ice impact on a panel and obtained

force histories. Sun et al. [13] designed a model based on a mass-spring-damper system to predict the peak force generated during ice impact onto a panel. The stiffness and the mass of the target were characterised by a spring and a lumped mass, respectively, and the values of stiffness were empirically fitted. The results gave a reasonable estimate for the peak force at a relatively low velocity range (*i.e.*, 10 m/s to 40 m/s).

The value of peak force depends on geometric and mechanical properties of both the impactor and the target, as well as the impact velocity. As a first step, it is interesting to study a simple case of an ice ball impacting onto a rigid target. As the peak force increases with the stiffness and mass of the target, this case of using a rigid target should provide an upper bound for the peak force, which is of critical importance in quantifying the mechanical response of panels in resisting the impact. Several studies have been performed for the peak force between an impactor and a rigid target [14-19] and most of them employed a load-cell as backing in order to capture the force history. Pereira et al. [16] tested the impact response of an ice cylinder on rigid target and obtained the force history generated using a piezoelectric load cell mounted on a circular sensor plate. They evaluated the effect of ice microstructure on the force history, including single-crystal, poly-crystal and low-density ice. The results indicated that the effect of ice microstructure on the peak force was minimal. Carney et al. [19] conducted similar impact tests by using the same setup as that of Pereira et al. [16] and then validated a phenomenological model considering failure, especially developed for ice impact. In addition to using plates, Combescure et al. [1] also studied the ice impact on a rigid target by using a piezoelectric load cell and no force history was provided, however.

Instead of using load cells, several studies attempted to obtain the force history by designing a force/impulse transducer system [17, 18]. The force was measured by using a quartz load cell washer sandwiched between a rigid backing plate and a top plate [17]. Ice balls were launched to the target at speeds from 60 to 90 m/s. The impulse measured was found to

be roughly equal to the input momentum, which indicated that the momentum loss due to the force impulse transducer (FIT) system could be neglected. Moreover, it was reported that the peak force was related to the kinetic impact energy by a power law regardless of the sizes of the ice balls. Kim and Kedward [18] used a system similar to FIT in order to record the force history of ice impacting on a rigid target. Monolithic ice balls and flat-wise layered ice balls were employed as the impactors. It was concluded that the influence of ice microstructure on the peak force could be negligible, as also observed in [16].

When a load cell or force impulse transducer is employed in high velocity impact, the accuracy of experimental data could be of concern. It is known that the velocity of shock wave propagation can be high and also sensitive to contact details in the load cell fixture. This may result in accumulation of iterative positive and negative waves in the measured time window, leading to reduced reliability for the data. The plate placed on the top of a load cell introduces an inertia effect, which reduces the force transmitted to the loadcell. To overcome these shortcomings, Tippmann et al. [15] used a modified Hopkinson bar to measure the force history. An ice ball was launched to one end of a hollow aluminium tube. Strain gauges were attached to measure the voltage signal generated by ice impact and the signal was converted to force history. This method eliminated the drawbacks of using a load cell. The peak force was found to be a function of the impact kinetic energy of the ice balls. Pernas-Sánchez et al. [20] compared the peak force obtained using a load cell with the data obtained by Tippmann et al. [15] and found that the peak forces measured by a load cell were slightly lower than those measured by strain gauges. Lower rigidity of the target due to the load cell may account for this difference. They also obtained a semi-empirical relationship which relates the peak force to the impact kinetic energy. Recently, Tan et al. [14] conducted impact tests using a Hopkinson bar to study the characteristics of layered ice under impact velocities. Layered ice was fabricated to simulate the natural hailstone due to its onion-like structure. The peak force

produced by layered ice was found to be higher than that for pure ice, probably because the layered structure might delay the disintegration of the ice ball in the impact.

Natural hailstones are formed by the freezing and attaching life cycle of water droplets in particular thunderstorm cells [21], which results in onion-like structures. For experimental studies, it is common to use laboratory-grown spherical ice to represent a hailstone due to the difficulty of replicating the exact forming environment of a natural hailstone. Since the properties of the impactor play an important role in an impact event, the mechanical properties of ice should be characterised first. The mechanical strength of ice is, however, considerably scattered due to its sensitivity to the microstructure and the temperature. The compressive strength of ice was found to be between 5 and 25 MPa from -10 °C to -20 °C [22]. The smaller grain size and lower temperature, the higher the compressive strength of ice [23]. The tensile strength of ice was found to be 2.14 MPa on average at -7 °C from the uniaxial tensile test [24]. Alternative to direct tensile test due to technical difficulties, some studies employed the Brazilian test as an indirect tensile test. Typical tensile strength of ice obtained in Brazilian tests ranged from 0.68 to 2 MPa [25], lower than that obtained in a direct tensile test. Moreover, the tensile strength of ice is significantly affected by the grain size with negligible strain rate sensibility [26]. Typical Young's modulus of ice was characterised as 3 to 10 GPa at -10 °C [27].

This study aims to quantify the peak force in the impact of an ice ball onto a rigid target and identify the parameters that affect the peak force (F_p) and time corresponding to the peak force (T_p). Ice balls frozen at -10 °C and -30 °C were prepared using a casting method. Quasi-static Brazilian tests were conducted to characterise the tensile strength of ice. Impact tests were conducted on a modified Hopkinson bar of 4 meters in length with a pair of strain gauges mounted on the surface, capable of recording the force history. The impact velocities ranged from 13 to 105 m/s. The effects of impact velocity, impactor size and temperature on F_p and

T_p were investigated. Dimensional analysis was conducted to find an empirical relationship for both F_p and T_p, with the impact velocity. Experimental data from the previous work by Tippmann et al. [15] and Tan et al. [14] were compared with the present study and they agree with the developed empirical relationships.

2. Quasi-static tests for tensile strength

2.1 Specimen preparation

A unique feature of the predictive expressions to be presented in the later part of the article is incorporating the tensile strength of ice as a modelling parameter. Thus, Brazilian tests were conducted to obtain the tensile strength of ice at -10 °C and -30 °C, respectively. In order to make bubble-free ice, a delicate method was used. Vacuum walled cans (Polar cans) of an inner diameter of 65 mm (Fig. 1a) were filled with clear tap water and then frozen for at least 44 hours without caps in a freezer (Meiling Ultra low temperature freezer DW-FL439). "Polar cans" may provide sufficient vacuum insulation along circumferential and bottom faces, guiding water to freeze unidirectionally from the top open surface to the bottom, which may force the resolved air in the water to escape towards the bottom when freezing. The ice was kept at two temperatures, *i.e.*, -10 °C and -30 °C, respectively. This process can make raw ice cylinders of approximately 65 mm in diameter, which were then delicately cut to specimens of 32.5 mm thick for Brazilian tests. Fig. 1b shows a typical ice cylinder fabricated by using this method.

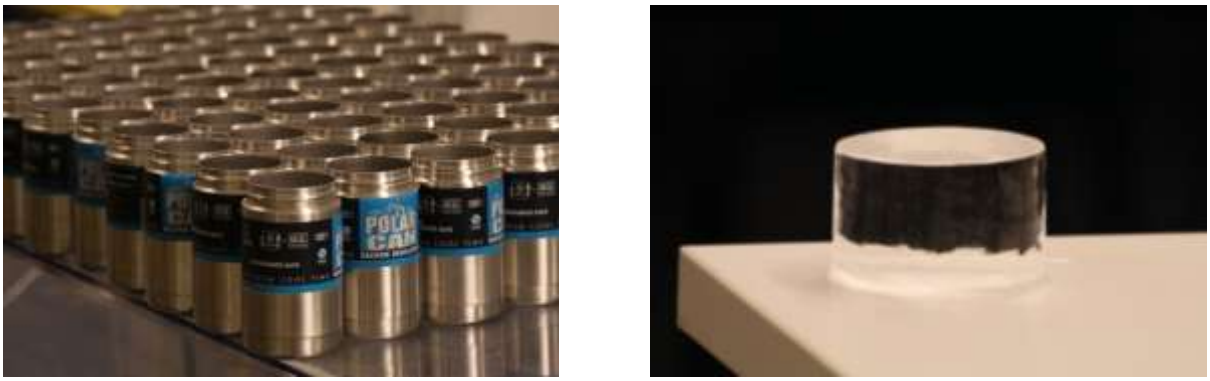

(a) (b)

Fig. 1. Preparation of cylindrical specimens: (a) "polar cans" for making clear ice cylinders; and (b) a clear ice cylinder for Brazilian test.

2.2 Experimental setup

Fig. 2a shows the setup of the Brazilian tests. The Brazilian tests were performed using an Instron 5965 at room temperature. A loading rate of 10 mm/min was employed for the purpose of shortening the test duration to mitigate the effect of temperature rise in tests. Polycarbonate sheets were inserted between the load platens and the specimen to minimise melting at the contact. All the ice specimens were loaded to failure within 30 seconds after taking out from the freezer.

2.3 Experimental results

It should be noted that the Brazilian test is only valid when specimens split from the middle at failure. Fig. 2b shows a typical specimen after failure, which is treated as a valid test. Three valid tests were obtained for -10 °C ice and four for -30 °C ice. The tensile strength is calculated by using Equation (1) [28, 29],

$$\sigma_T = \frac{2F}{\pi D t} \quad (1)$$

where F is the peak force obtained from the tests, D is the diameter of the disc, and t is the thickness of the sample.

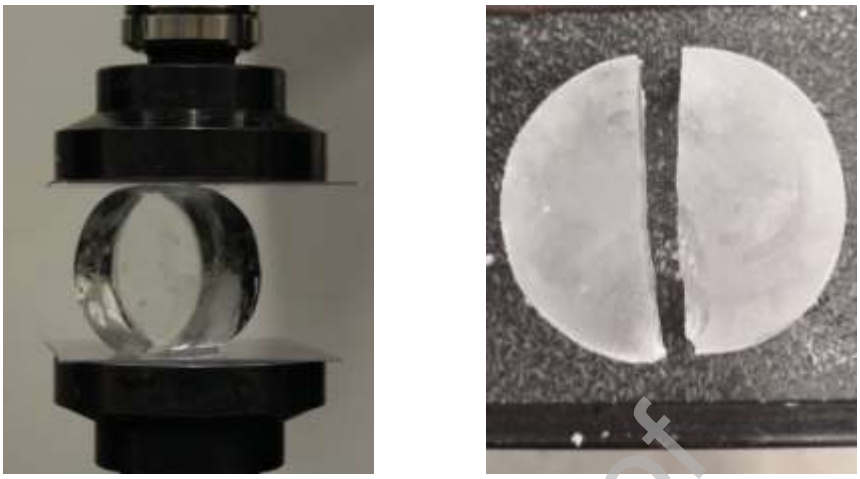

(a) (b)

Fig. 2. Brazilian test: (a) an ice sample was loaded between two platens insulated with polycarbonate sheets, and (b) a typical fractured specimen after test.

Fig. 3a and 3b show the force-displacement curves obtained from the Brazilian test for ice at -30 °C and -10 °C, respectively. The tensile strengths obtained are shown in Fig. 4, which are calculated as 0.69 MPa for -30 °C ice and 0.56 MPa for -10 °C ice on average. Although the obtained data in tensile strength varies within a range of 7% for -30 °C ice and 11% for -10 °C ice, respectively, the average tensile strength is close to that obtained by Mellor and Hawkes [25], which was approximately derived as 0.5 MPa for -7 °C ice. Moreover, the tensile strength slightly increases with decreasing temperature [30].

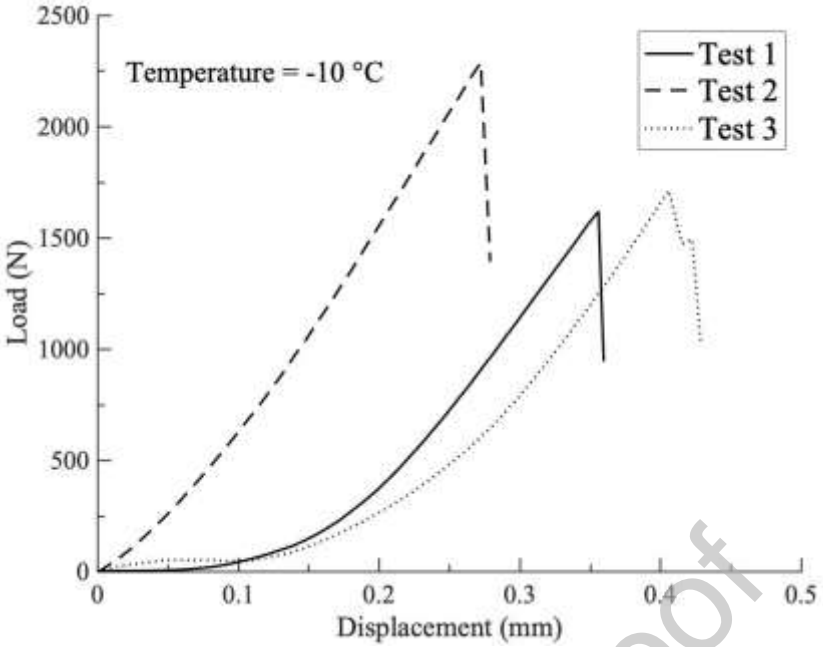

(a)

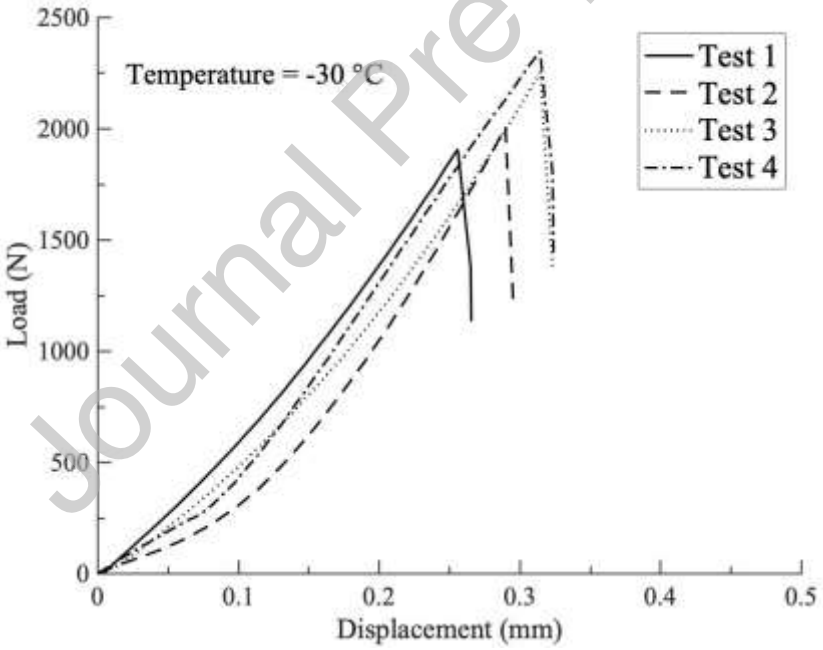

(b)

Fig. 3. Force-displacement curves obtained from the Brazilian tests (cross-head speed: 10mm/min): (a) for -10 °C ice, and (b) for -30 °C ice.

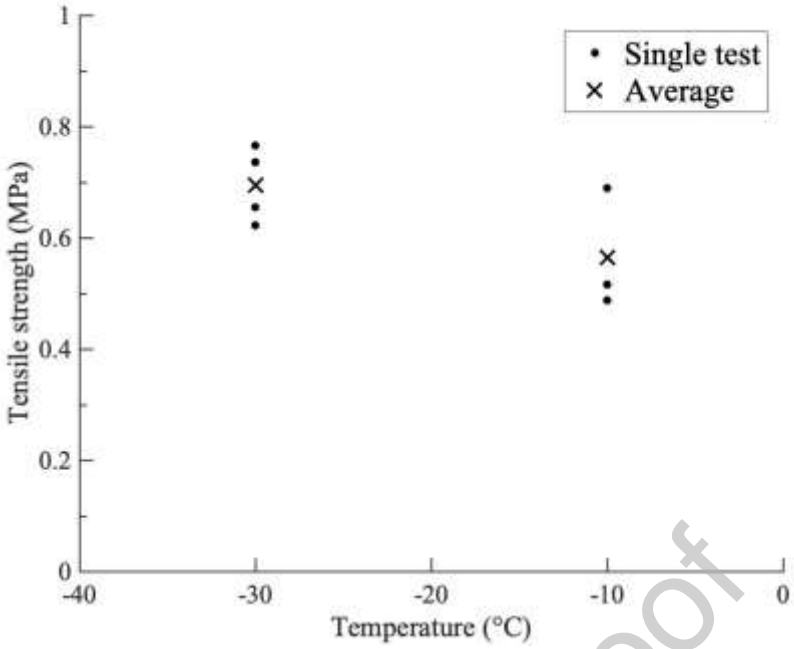

Fig. 4. Tensile strength of fabricated ice frozen at -10 °C and -30 °C.

3. Impact tests

3.1 Specimen preparation

Spherical ice specimens with a diameter of 50.8, 44.5, 38.1, and 31.8 mm were prepared by using self-designed moulds, as shown in Fig 5a. The corresponding values of mass were 58.0, 40.5, 25.2, and 14.4 g. The fabrication process for ice was the same as that for Brazilian tests. Clear ice without bubbles was obtained by freezing tap water in the "Polar cans" and then maintained at -10 °C or -30 °C for at least 44 hours. It was then sandwiched between the two parts of the mould with a pre-machined spherical inner surface. The ice melted due to the heat transfer from the moulds and was gradually pressed into a perfect spherical ball under the self-weight of the top cap, guided by two columns. The ice ball was then immediately placed in the freezer again at the set temperature of -10 °C or -30 °C for another 24 hours. A crystal clear spherical ball is shown in Fig. 5b.

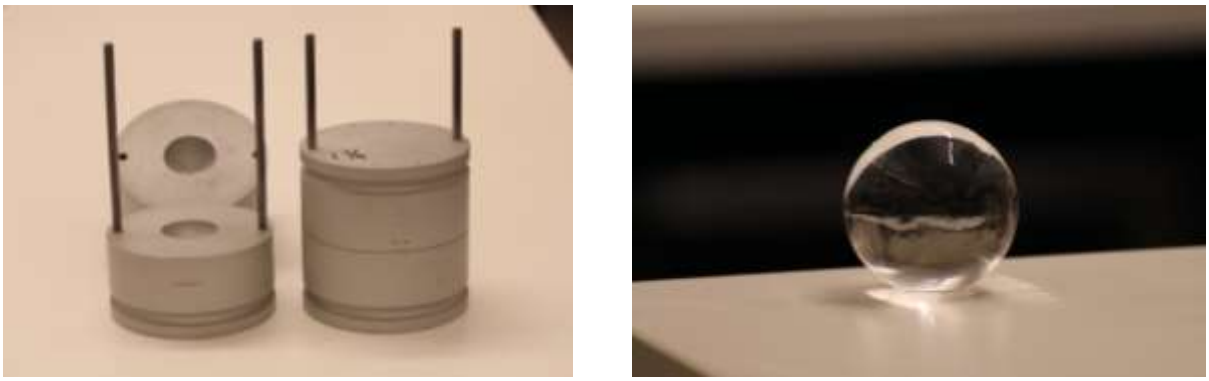

(a) (b)

Fig. 5. Preparation of spherical ball: (a) moulds for forming ice balls with different diameters, (b) a crystal clear spherical ice for the impact test.

3.2 Experimental setup

Fig. 6a and 6b show the setup of the impact test and its sketch, which was modified from a split Hopkinson pressure bar with a gun barrel of 37 mm in diameter. A compressed air launcher was used to shoot an ice ball specimen to the end cross-section of an aluminium bar of four meters in length, which effectively avoided any interference of wave pulses reflected from the far end within the impact time period. Compressed nitrogen gas was used. By controlling the pressure of the gun, different impact velocities were achieved. In order to accommodate spherical ice balls of different sizes, a 0.5 meters long PVC extension tube was connected to the existing steel gun barrel, and specimens were placed into position through a cut-off hole on top of the PVC tube adjacent to the end of the barrel. Pressure gas accelerated the ice specimen in the extended PVC tube to achieve desired velocities. PVC extension tube was used to minimise possible melting of the specimen. The time interval between placing the specimen and firing the gun was within one minute so that the temperature of the ice ball did not change considerably. Aluminium bar of 70 mm in diameter was selected as the target for its relatively low value of Young's modulus, which was measured as 67.6 GPa. Its density was 2673 kg/m^3. A pair of semiconductor strain gauges with gauge factor of 110 and resistance of

130 Ω were mounted on the surface of the bar at 0.9 m from the impact end. During the impact, voltage signals in the Wheatstone bridge through a half bridge connection were firstly amplified and then recorded by an oscilloscope (Tektronix TDS 2024B). The impact velocity was measured by a high-speed camera (Phantom V2512) placed perpendicular to the flying path of the ice balls. The exposure duration of the specimen in environment temperature averaged approximately 45 seconds. The mass of each specimen was measured by a digital scale before launching. The fragmentation process of the ice ball was captured by high speed photography at a frame rate of 52,000 frames per second.

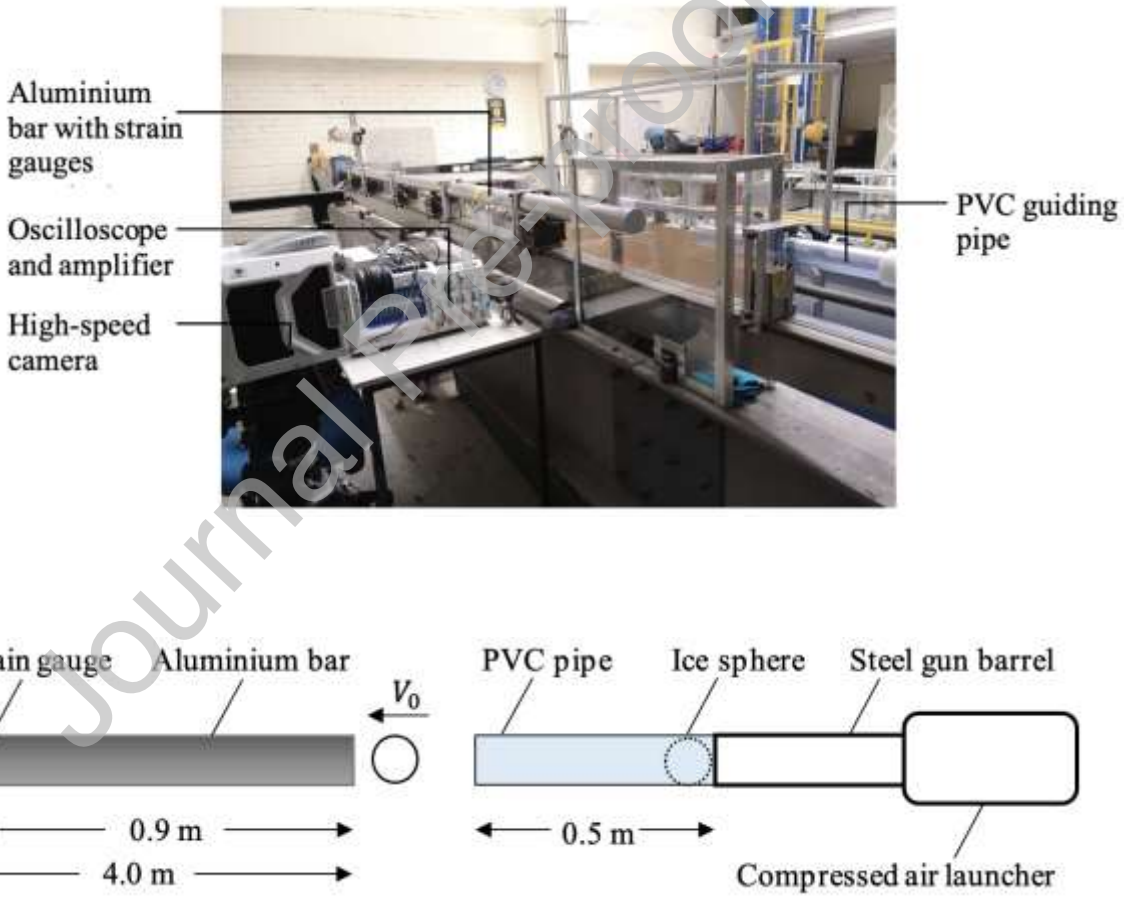

Fig. 6. Experimental set-up for the impact test: an ice ball is launched onto the end cross-section of an aluminium bar with velocity V_0 through the PVC pipe. (a) a photograph, and (b) a sketch

3.3 Data processing

The original voltage signals recorded in the oscilloscope were low-pass FFT filtered at a cut-off frequency of 50 kHz, which did not evidently change the magnitude of the peak force. The strain history was converted from the voltage history by using a calibrated voltage to strain coefficient of 60.6 με/V. With the measured Young's modulus and cross-section area of the aluminium bar, the force history was calculated by using Hooke's law in the elastic range. A total of 149 tests were conducted and there were 80 force histories obtained for -10 °C and 69 for -30 °C at impact velocities ranging from 13 to 105 m/s. Note that typical terminal velocity of natural hailstones ranges from 5 m/s to 50 m/s. The selected velocities largely cover this range. The test rig could not produce repeatable velocities at lower velocities. The selection of higher velocity up to 105 m/s is also because of potential applications in aerospace industry.

3.4 Fragmentation process and typical force histories

The fragmentation process of an ice ball was imaged every 19.23 μs by a high-speed camera. Fig. 7 shows the frames captured within the first 1 ms after the initial contact, for a 50.8 mm ice ball impacting at 68.5 m/s. The ice ball is clear and transparent before the initial contact, followed by crack initiation and propagation in a very short period. At 19.23 μs, the crack propagated to roughly 3/4 of the diameter and then completely through the ball between 19.23 μs and 38.46 μs. The crack propagation speed was estimated at 1,834 m/s, which is comparable to that observed by Combescure et al. [1], *i.e.*, 2000 m/s.

Fig. 8 shows the force history of the above specimen. At 72 μs after the initial contact, the force reached its maximum value of 17 kN and the deformation was close to the photograph at 76.92 μs in Fig. 7. Evidently, cracks were spreading throughout the ball at this instant, when the specimen was in the process of disintegration. The force decreased sharply when severe fragmentation occurred. At 500 μs, the ice ball completely disintegrated to tiny debris,

behaving like granular fluid. The corresponding force at this time was only 20% of the peak force. At 1000 μs, the force further decreased to less than 0.5 kN and the ice debris continued spreading radically, approaching the end of the impact process.

① t = 0 μs ② t = 19.23 μs ③ t = 38.46 μs

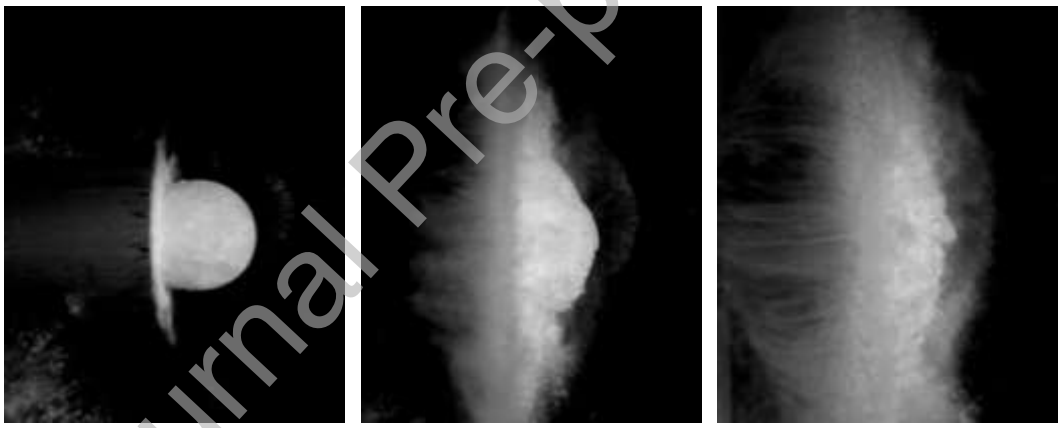

④ t = 76.92 μs ⑤ t = 500 μs ⑥ t = 1000 μs

⑦ t = 2462 μs

(a)

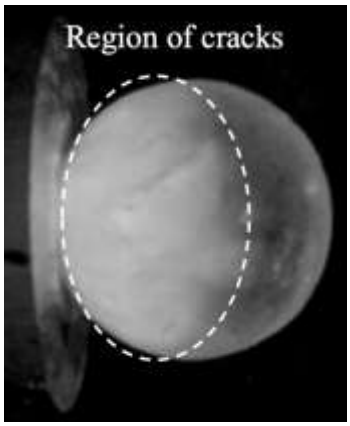

(b)

Fig. 7. (a) The fragmentation process of a 50.8 mm ice ball impacting at 68.5 m/s. (b) Enlarged view of the ice ball showing cracks at t = 19.23 μs.

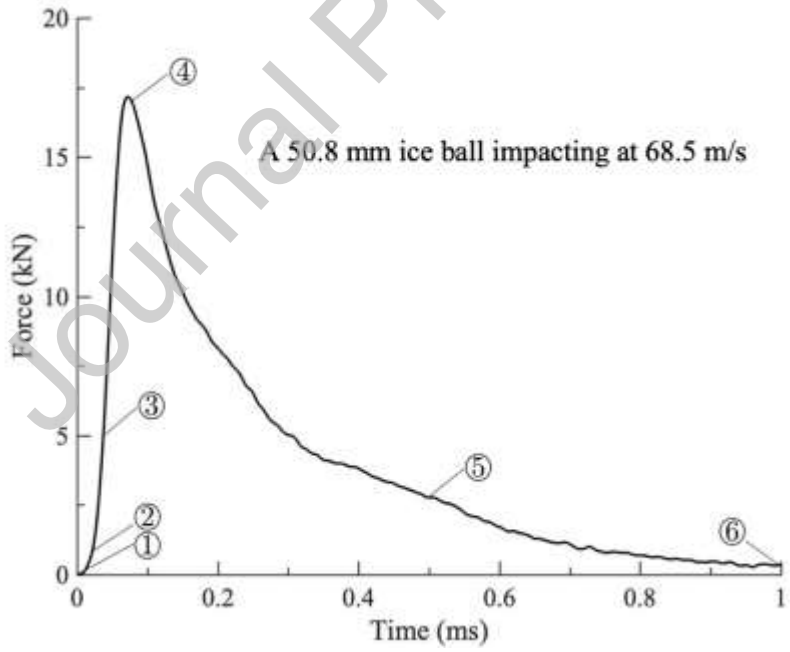

Fig. 8. Typical force versus time history. Diameter of the ice ball is 50.8 mm and the impact velocity is 68.5 m/s.

3.5 Typical experimental results

Fig. 9a shows the force histories of 50.8 mm ice balls (frozen at -30 °C) impacting at different impact velocities. All the curves exhibit similar features as in Fig 8. With the increase of impact velocity, the peak force, F_p, increases significantly, while the time reaching the peak force, T_p, increases slightly. Fig. 9b shows the force histories of ice balls of different diameters, all for a given temperature of -30 °C and impact velocity of 60 m/s. It shows that both F_p and T_p increase with the diameter (and hence mass) of the balls. Increasing velocity and mass of the ball leads to enhanced momentum of the ball, and this results in higher peak forces.

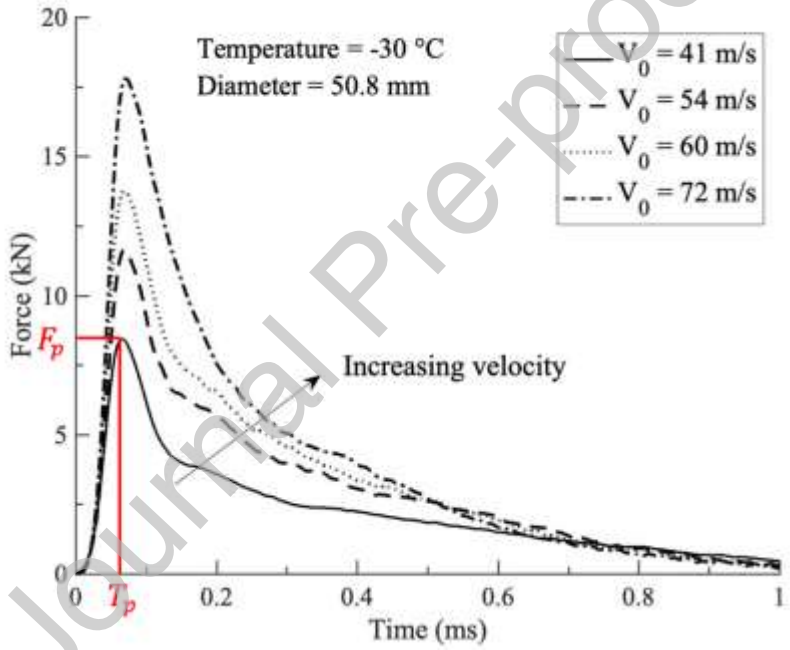

(a)

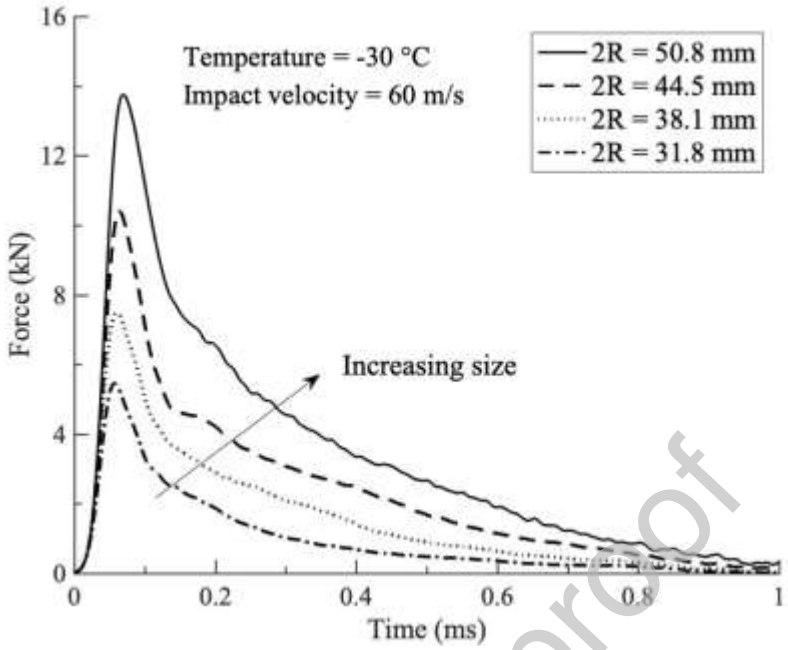

(b)

Fig. 9. Force histories: (a) 50.8 mm-diameter ice balls impacting at different velocities (-30 °C), and (b) ice balls of different diameters at the same impact velocity of 60 m/s (-30 °C).

Fig. 10 shows the force history of ice balls, which have the same diameter of 50.8 mm but different frozen temperatures at -10 °C and -30 °C, respectively. Two impact velocities, 73.0 m/s and 34.6 m/s, were employed for the two types of ice balls. The results show that, at both the velocities, the peak force for ice balls at -30 °C is approximately 15% higher than that at -10 °C. On the contrary, ice frozen at -10 °C takes slightly longer time to reach the peak force, *i.e.*, a larger value of T_p. The *F-t* curves also show a slightly steeper curve before the peak for ice frozen at -30 °C.

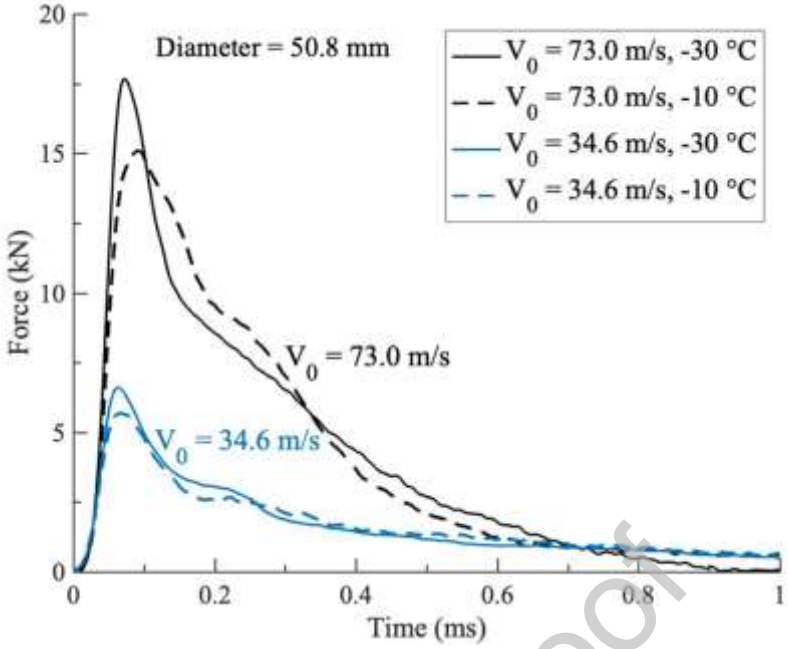

Fig. 10. Force histories of 50.8mm ice balls at impact velocities of 73.0 m/s and 34.6 m/s, prepared at -10 °C and -30 °C.

4 Dimensional analysis and empirical formulae

The three key parameters of interest are the peak force, the time corresponding to the peak force and the impulse generated from the impact. Once these are known for any impact scenario, subsequent structural responses could be estimated. Note that these values for impact onto a rigid and heavy target represent an upper bound for other scenarios of ice ball impact onto a structure with a finite stiffness and mass. Here we present a dimensional analysis for the data from a total of 149 tests conducted.

4.1 Peak force

The peak force is plotted against the impact velocity for ice balls of four different values of diameter, in Fig. 11a for -10 °C ice and Fig. 11b for -30 °C ice. Generally, the peak force increases with the impact velocity regardless of size and frozen temperature of the ice balls. However, lower frozen temperature results in slightly higher peak force.

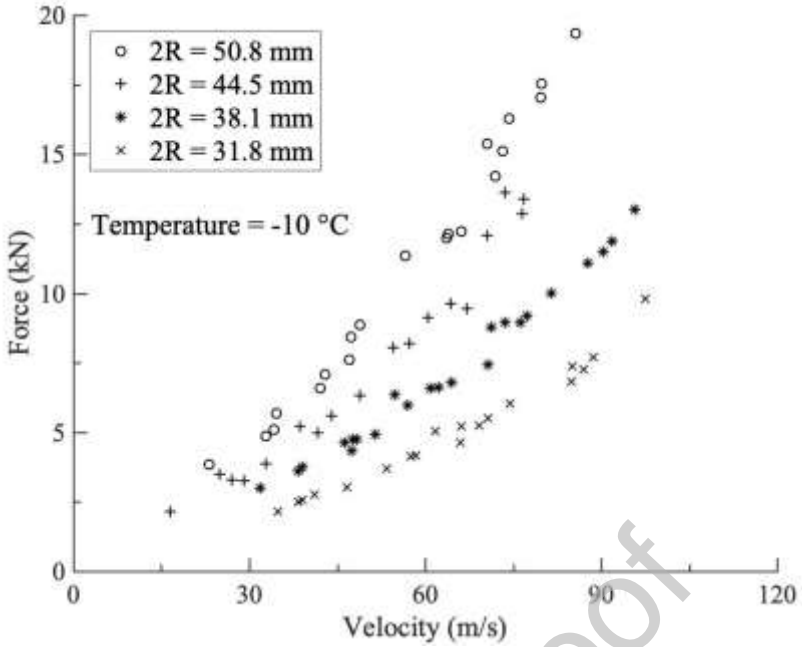

(a)

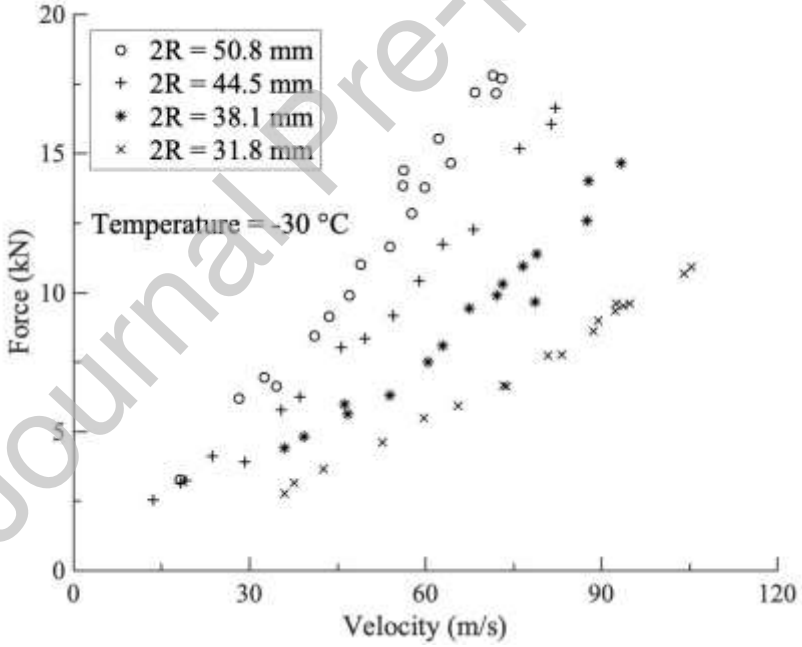

(b)

Fig. 11. Peak force vs. impact velocity for ice balls of different sizes: (a) -10 °C ice; (b) -30 °C ice.

Fig. 11 also shows that the peak forces are highly dependent on three factors, size of the ice balls, frozen temperature and impact velocity. It is also observed that the peak force is

monotonically related to an individual parameter if the other two parameters are fixed. Hence, it is likely that one single formula could be developed to describe all these relationships, which is not available in literature. Here, dimensional analysis is conducted to establish an expression for the peak force of ice impacting on a rigid target.

In this study, the aluminium bar can be regarded as a rigid target for its large mass and significantly higher value of elastic modulus than that for ice. Therefore, the bar's dimensions and properties are irrelevant. Other parameters that may affect the peak force F_p, are the radius of the ice ball (R), the impact velocity (V_0), the tensile strength of ice (σ_T) and the elastic wave velocity (c). The values of Young's modulus, tensile strength and density for ice at two different temperatures are given in Table 1. The following equation involving five physical variables can be written,

$$f\left(F_p, R, V_0, \sigma_T, c\right) = 0 \tag{2}$$

Table 1. Material properties of ice employed in the dimensional analysis

Temperature (°C)	Young's modulus (GPa)	Tensile strength (MPa)	Density (kg/m^3)
-10	5	0.56	870
-30	5	0.69	870

Based on the Buckingham theorem [31], the number of independent dimensionless groups can be obtained as the difference between the number of physical variables and the number of basic dimensions. In this impact problem, the three basic dimensions involved are

length, mass and time. Therefore, there are two independent dimensionless groups (5 – 3 = 2), which can be identified as $F_p/(R^2\sigma_T)$ and V_0/c. In the initial stage of this analysis, only tensile strength for -10 °C was measured as σ_T = 0.56 MPa and this value was used for both the two temperatures in the dimensionless plot in Fig. 12. Note that this is a double logarithmic plot. It should be noted that the elastic wave propagation speed, *c*, is calculated by $\sqrt{E/\rho}$ (where E is the Young's modulus of ice, taken as 5 GPa [27], and ρ is the density of ice, taken as 870 kg/m^3 measured from the experiments), which is 2397 m/s. It can be seen that all the experimental data points are now condensed into two groups each with a different frozen temperature for the specimens.

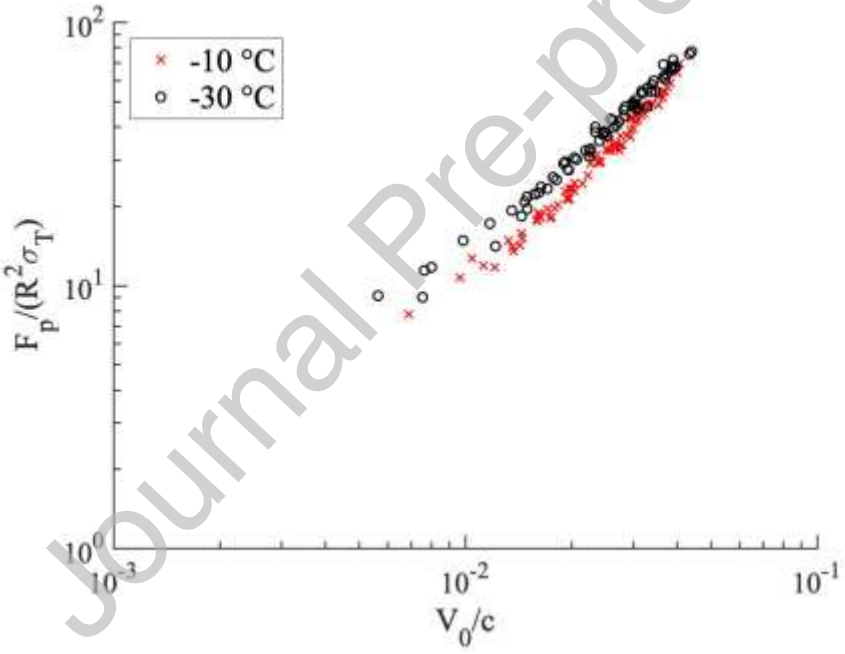

Fig. 12. Dimensionless peak force vs. dimensionless impact velocity for ice balls frozen at -10 °C and -30 °C (σ_T = 0.56 MPa for both temperatures)

In order to further understand the effect of temperature in the above plot, additional Brazilian tests were conducted for ice at -30 °C, which gave the value of tensile strength of 0.69 MPa. Therefore, different values of the tensile strength corresponding to the temperature were used in the dimensionless force and they are plotted in Fig. 13. Interestingly, now all the

data points covering various values of the parameters are condensed to one group. At this stage, we can say that the dimensional analysis is successful. To obtain an empirical formula, the points can be approximated by a straight line in this double logarithmic plot, which indicates a power law relationship in Equation (3).

$$\frac{F_p}{R^2\sigma_T} = 3969\left(\frac{V_0}{c}\right)^{1.31} \tag{3}$$

The values of the two coefficients in the above equation are obtained by best fitting technique. The above equation can be re-written in terms of the peak force and other parameters. Consequently, the peak force can be predicted by using a single formula, as follows

$$F_p = 3969R^2\sigma_T c^{-1.31}{V_0}^{1.31} \qquad 13\ m/s < V_0 < 105\ m/s \tag{4}$$

This suggests that the peak force is proportional to radius squared, quasi-static tensile strength, and impact velocity raised to a power of 1.31. The effect of Young's modulus and density of the ice is reflected through the elastic wave speed c.

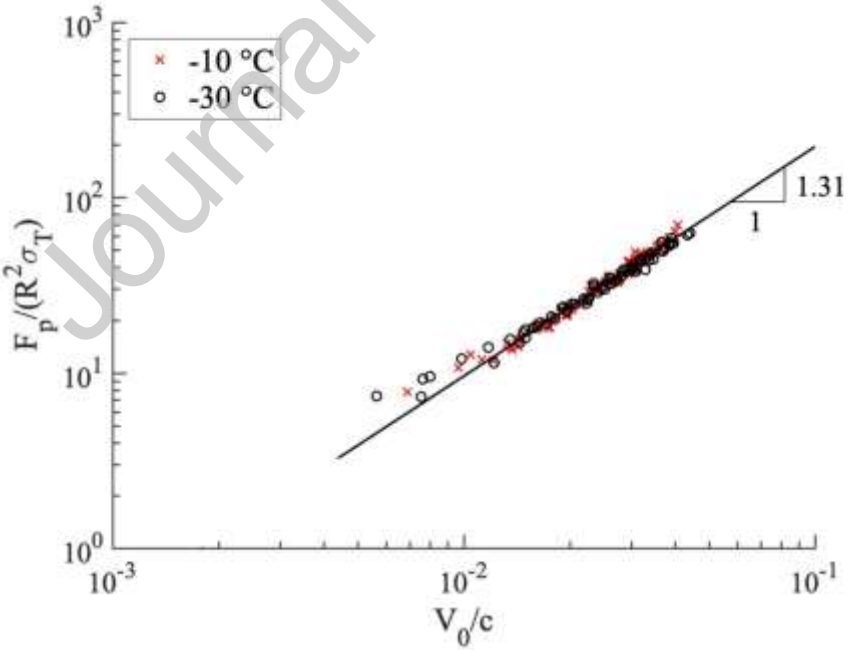

Fig. 13. Dimensionless peak force vs. dimensionless impact velocity for ice balls (σ_T= 0.56 MPa for -10 °C ice, 0.69 MPa for -30 °C ice).

4.2 Time corresponding to the peak force

Fig. 14 shows the influence of impact velocity, size and frozen temperature of ice on T_p. Although in general monotonically increasing trend for individual test group can be observed, the overall data seem rather scattered. From this figure, for specimens frozen at both the temperatures T_p increases with increasing impact velocity, by approximately 30% when velocity changes from 30 m/s to 90 m/s. The data for -10 °C ice is relatively scattered as compared with that of the -30 °C ice. It can be seen that T_p becomes larger when the diameter increases. Overall, at relatively low impact velocities ranging from 20 m/s to 40 m/s the temperature seems to have a minor effect on T_p, and the value of T_p is between 0.05 ms and 0.08 ms. When impact velocity is larger than 60 m/s, T_p is over 0.08 ms for -10 °C ice. However, it remains smaller than 0.08 ms for -30 °C ice. Overall, it takes longer time for the force to reach the maximum value for ice balls at -10 °C than at -30 °C.

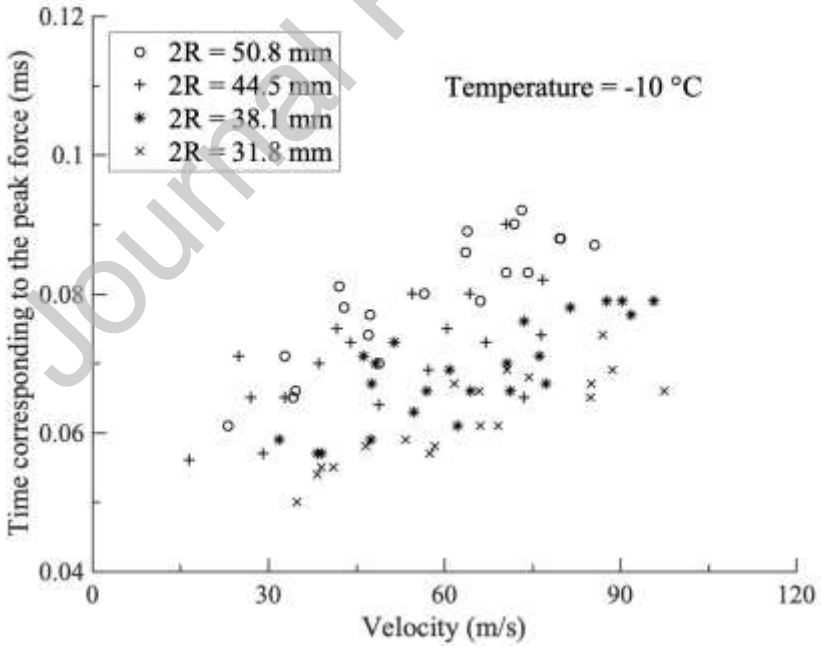

(a)

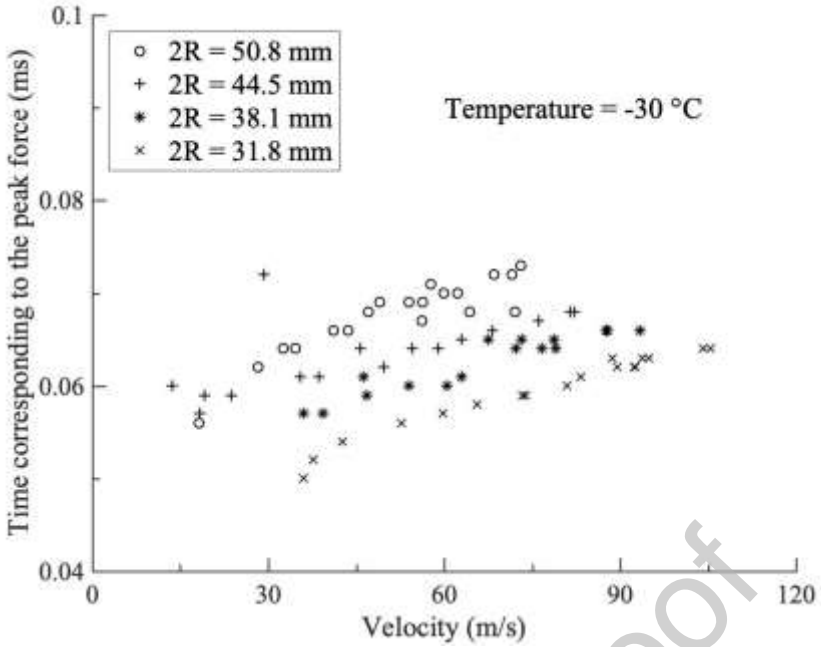

(b)

Fig. 14. Time corresponding to the peak force vs. impact velocity: (a) -10 °C ice; (b) -30 °C ice.

Similar to the earlier dimensional analysis, the time corresponding to the peak force T_p can be analysed. There are five physical variables in the dimensional analysis for T_p, *i.e.*, the time corresponding to the peak force (T_p), the radius of the ice ball (R), the impact velocity (V_0), the density of ice (ρ), and the tensile strength of ice (σ_T). Therefore,

$$f\left(T_p, R, V_0, \rho, \sigma_T\right) = 0 \tag{5}$$

Again there are three fundamental dimensions; mass, time, and length. Two independent dimensionless groups (5 – 3 = 2) can be found and we use $T_p/(R/V_0)$ and $\rho {V_0}^2/\sigma_T$. Fig. 15 plots the two dimensionless groups. Initially, the same value of σ_T of 0.56 MPa was used for all the points. Two distinct groups of points may be seen and the points for -10 °C are slightly higher than those for -30 °C.

To reconcile the difference, applying the respective values of tensile strength measured *i.e.*, 0.56 MPa for -10 °C ice and 0.69 MPa for -30 °C ice, the dimensionless T_p against the

dimensionless V_0 is plotted in Fig. 16. It can be seen that the two groups of data points are also condensed in a narrow band, similar to that for the peak force. This again shows that the dimensionless analysis is successful. The empirical relationship can be obtained by fitting the data using a straight line in the plot, which means a power law relationship,

$$\frac{T_p}{R/V_0} = 0.07\left(\frac{\rho {V_0}^2}{\sigma_T}\right)^{0.68} \tag{6}$$

This can further be written as

$$T_p = 0.07 R \rho^{0.68}\, {\sigma_T}^{-0.68} {V_0}^{0.36} \qquad 13\ m/s < V_0 < 105\ m/s \tag{7}$$

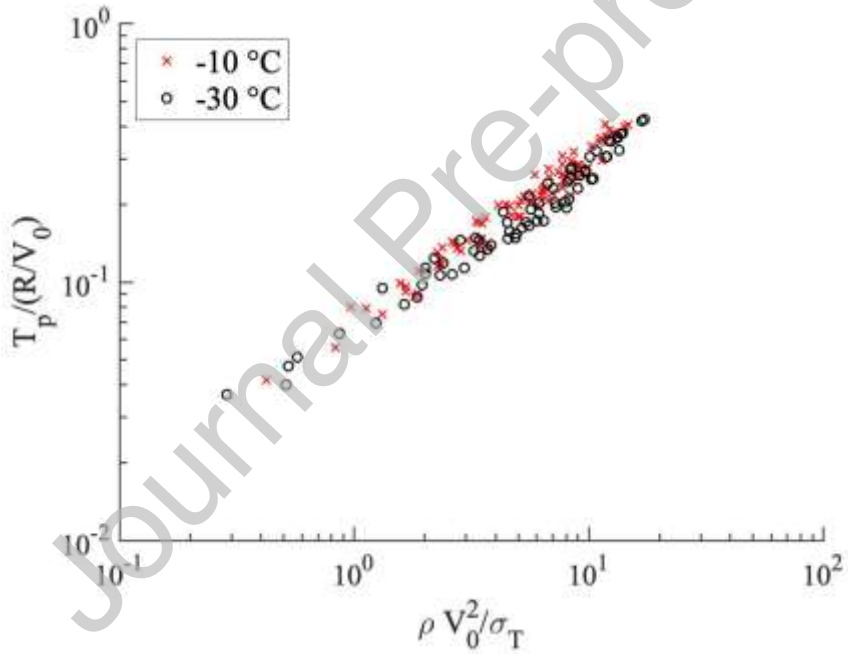

Fig. 15. Dimensionless time corresponding to the peak force vs. dimensionless impact velocity (σ_T = 0.56 MPa for both temperatures)

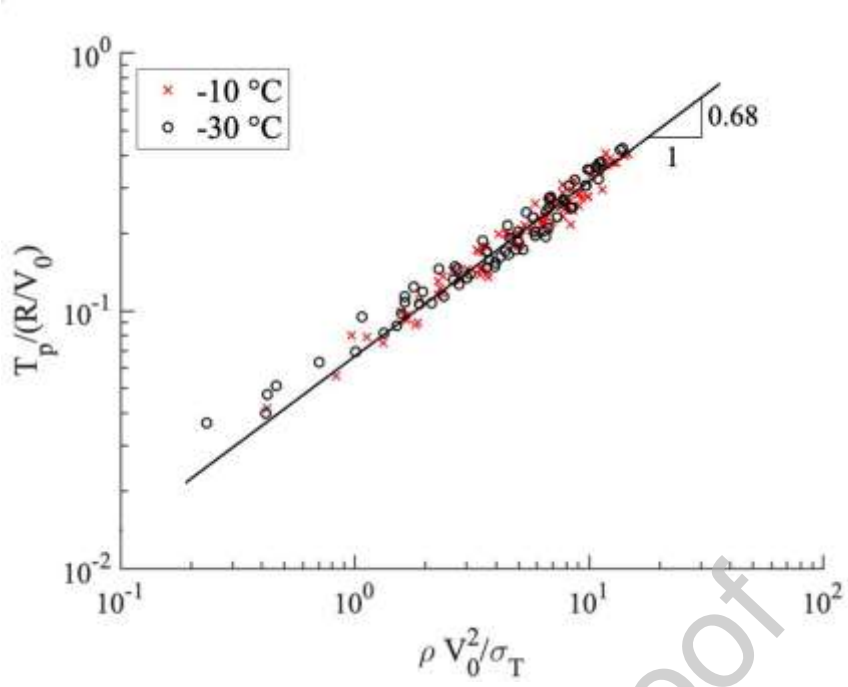

Fig. 16. Dimensionless time corresponding to the peak force vs. dimensionless impact velocity (σ_T = 0.56 MPa for -10 °C ice, 0.69 MPa for -30 °C ice)

4.3 Impulse and momentum

In an ideal impact process, the momentum of ice ball shall be fully converted to impulse measured, which is obtained by integrating the force-time curves. The present study investigates the relationship between the incoming momentum MV_0 and the impulse I in the impact of ice balls. M is mass of the ice ball. Fig. 17 plots the ratio of impulse measured to momentum, which shows the values vary between 0.8 and 1.12, being close to 1. A similar phenomenon was found by Singh et al. [17]. With the increase of impact velocity, the value of I/MV_0 increases slightly. The fact that the impulse is higher than the input momentum would suggest rebounding of ice fragments (also shown in Fig 7). For low velocity impact, the aluminium bar may not be long enough to capture the entire duration of the force during the tests, resulting in a very small amount of impulse not recorded. As illustrated in Fig. 10, for the impact of 34.6 m/s, the force was still only approaching to zero at 1 ms. This loss is much smaller for high velocity impact when the complete process finished at a much shorter duration.

However, this occurred at very late stage of impact and should not affect the values of peak force and the corresponding time analysed earlier. It is also possible that at low velocity impact, some fragments outside the cross-section of the bar kept moving forward, resulting a low impulse than the momentum. As values of I/MV_0 fall within 0.8 to 1.12 for all the impact tests, it may be concluded that the impulse is approximately equal to the incoming momentum of the ice balls.

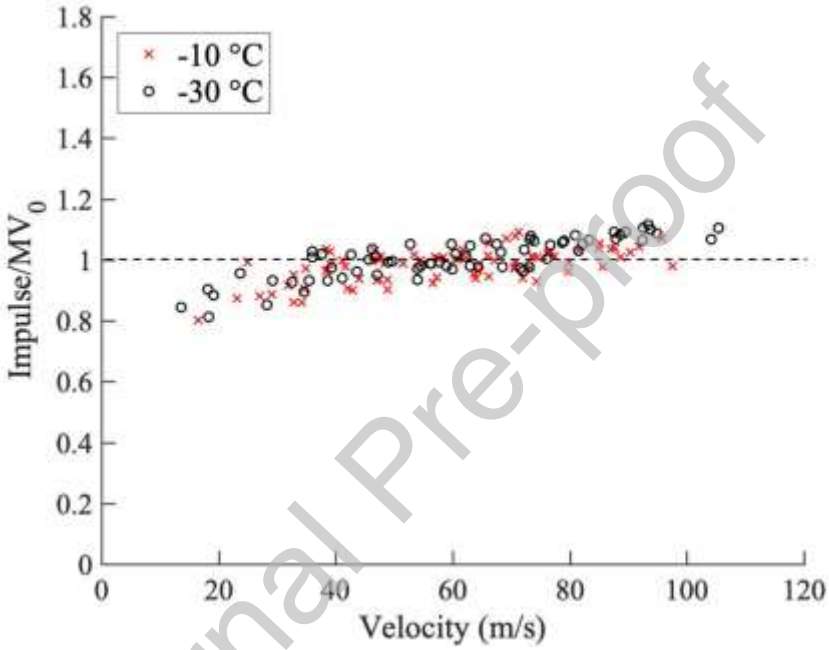

Fig. 17. The ratio of impulse/momentum for all the 149 tests. The average value is 0.97.

5 Discussion

5.1 Disintegration and failure mode of the ice ball

As a brittle material, the dynamic deformation and fracture of ice is complex and the associated studies can be a separate research area. Initially, the contact between the ice ball and the rigid target can be described as Hertzian contact [32], where compressive failure may take place. After the crack initiation and propagation through the ice ball, though the front part could be still experiencing compressive stress in the impact direction, the large back part of the ball

starts to disintegrate and expands radially, perpendicular to the impact direction. The fragmentation stage of the ice ball may involve compressive, tensile or shear failure. However, the exact mechanism needs to be understood in future. It should be noted that the mechanical strength of ice balls can only be retained before disintegration and it will be lost during fragmentation into debris. Therefore, both momentum and mechanical properties of the ice ball determine the behaviour of the ball before disintegration. The peak force is reached at an early stage of the disintegration. As the contact force surpasses the peak and starts to subside (as the ice specimen disintegrates), the rest of the time-history is controlled by the conservation of momentum principles. However, it is difficult to accurately monitor the forcing function by the high-speed camera during the phase of disintegration.

5.2 Comparison of the proposed empirical relations with previous results

A large number of data were obtained experimentally by Tippmann et al. [15] and Tan et al. [14] and they are plotted together with our data and the established empirical relations in Fig. 18. The properties of ice used for the present dimensional analysis are listed in Table 2. Note that the temperature of the ice tested was -20 °C and -18 °C, respectively, in the two studies. However, no experimental tensile strength of the ice was given in either of the investigations. In Tippmann et al., the value of the tensile strength was chosen as 0.517 MPa in the finite element analysis, which gave the best correlation between the numerical results and the experimental data. Therefore, the average value for -10 °C and -30 °C from the present tests, *i.e.*, 0.625 MPa, is used. For the range of low-to-medium velocity impact, the data obtained by Tippmann et al. [15] and Tan et al. [14] are in a good agreement with the present empirical formula. At high impact velocity, the present equation underestimates the results slightly. Given the large scatters observed in their results, it may still be said that the present equation can give a good estimate for the peak force. Previous experiments were conducted by the present group [13], where an ice ball impacted onto a rigid mass supported by an elastic

spring. Even though the setup was different, it would be interesting to plot the data also as shown in Fig. 18. The value of tensile strength for -10 °C from the present tests, *i.e.*, 0.56 MPa, is used for [10] as the specimens were prepared at a temperature within the range of 0 to -10 °C. The data points fall broadly with the same trend, slightly lower values than the data obtained by present study, but a little higher than the fitted curve in lower velocity range. This difference is reasonable given that the mass which was supported by the spring was much smaller than the Hopkinson bar.

Unfortunately, the prediction of peak time cannot be verified due to lack of data in literature. In the work by Tippmann et al. [15] the obtained data for T_p was dramatically scattered. In the work by Kim et al. [18], no noticeable trend was observed. Due to the complex nature of ice impact, the results might be affected by multiple parameters and it is challenging to obtain consistent results.

Table 2. Material properties of ice employed to analyse the peak force in literature. The average value for -10 °C and -30 °C from the present tests, i.e., 0.625 MPa, is used for [11] and [12]. The value for -10 °C from the present tests, i.e., 0.560 MPa, is used for [10].

Reported study	Young's modulus (GPa)	Tensile strength (MPa)	Density (kg/m^3)
Tippmann [15]	5	0.625	880
Tan [14]	5	0.625	867
Sun [13]	5	0.560	870

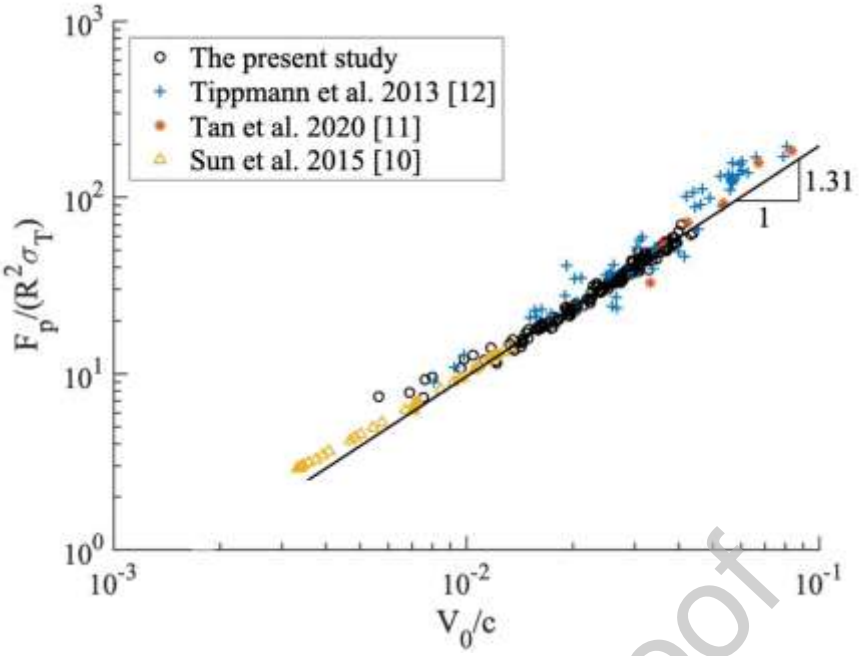

Fig. 18. Comparison of the present empirical relationship for dimensionless peak force with the previous studies

5.3 A note on force history characterisation

For both the dimensionless plots of F_p against V_0 and T_p against V_0, all the data agree well with the empirical relationship established for the velocity range studied. With the present formulae, the peak force and time corresponding to the peak force can be predicted beforehand for each impact case with known velocity and size of the ice balls. The impulse, which is the area under force-time curve, can be approximately regarded as the same value as the incoming momentum MV_0 of the impact. Therefore, if the force history for a specified ice ball can be approximated as a triangle with F_p being the height, knowledge of F_p, T_p and the area of this triangle would uniquely determine the force history, as shown in Fig 19a. It would be interesting to estimate the impulse corresponding to the stage when force is assumed to be increasing up to the peak value, called "first stage". Hence, from the established empirical formulae for peak force and time,

$$\frac{\frac{1}{2}F_pT_p}{MV_0} = 33.2{\sigma_T}^{0.32}E^{-0.655}\rho^{0.355}{V_0}^{0.67} \tag{8}$$

For ice at -30°C, using corresponding values for strength and density, we have empirically

$$\frac{\frac{1}{2}F_pT_p}{MV_0} = 0.012{V_0}^{0.67} \tag{9}$$

This indicates that the ratio of initial stage impulse increases with the initial impact velocity, as also plotted in Fig 19b, from 10% to 25% for the range of velocities tested.

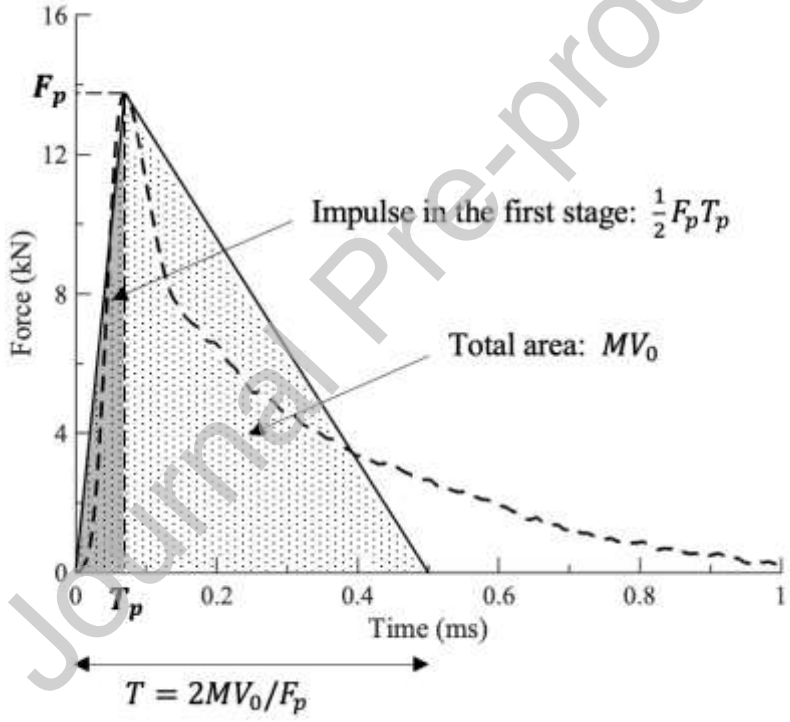

(a)

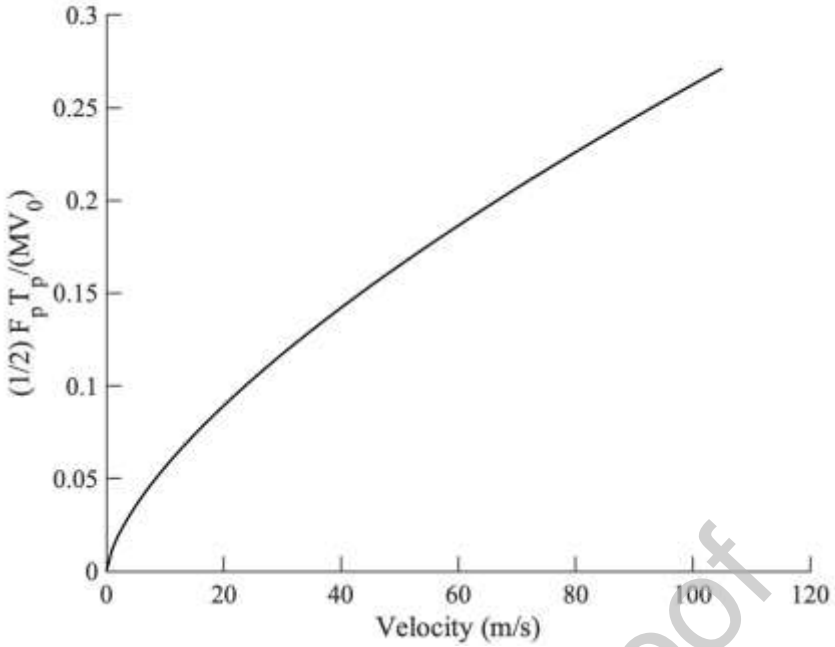

(b)

Fig. 19. (a) Simplified force-time straight lines. The stage of force increasing is defined "first stage" and the total area underneath the two straight lines is assumed as being equal to the initial momentum; (b) Plot of the first stage impulse normalised with initial momentum vs. velocity.

It should be mentioned that the present study mainly focuses on an ice ball impacting onto a rigid target. However, previous studies have shown that the contact force between an impactor and target could also be significantly affected by the mass and stiffness of the target [13, 33-35]. Therefore, the characteristics of impact target should be incorporated into future experimental studies.

5.4 Merits of incorporating tensile strength as parameter in the predictive expression.

The incorporation of tensile strength (of the ice specimen) as a modelling parameter, in lieu of temperature, is that tensile strength is more direct in representing the mechanical properties of hail affecting its contact force behaviour; and can be obtained conveniently by quasi-static testing of the ice specimen. The parameter of tensile strength takes into account of the effect of the temperature and ice microstructure. The tensile strength parameter featured in

the proposed expression can be used in future modelling work for encapsulating the effects of the void ratio and internal structure of a real hailstone on the peak contact force by one parameter.

A note of caution is also made here. Dimensional analysis requires a parameter with unit of stress/strength to be used. Ideally, that parameter should characterise the main physics of the exact failure and fragmentation mechanism under impact loading. In the absence of such knowledge, we have used the most common parameter, tensile strength, which would suggest an implicit hypothesis of tensile failure. The fact that when tensile strength is used, both the peak force and the time corresponding to the peak force can be perfectly fitted into one empirical relationship, respectively, regardless of temperature and size of ice balls may suggest that our hypothesis is reasonable. If cracks are found to be dominated with shear cracks, then shear strength would be more relevant. The shear strength is usually related to tensile strength and hence the empirical formulae would still be applicable, but with a different value for coefficient.

It should also be noted that the tensile strength of ice is reported to be insensitive to the strain rates in the low range of from 10^{-7} to 10^{-3} s^{-1} [36]. Further investigation may be necessary to study possible strain rate effect on the tensile properties of ice in the higher range, which has not been reported in literature. Moreover, mechanisms of fracture and fragmentation of the ice ball need detailed investigations. Depending on the exact mechanism, an appropriate parameter for strength may be used in the proposed empirical relations, such as compressive strength and shear strength of ice .

6 Conclusion

In this paper, clear ice balls and cylinders were made by moulding and then stored at -30 °C and -10 °C. Brazilian tests were conducted to obtain tensile strength of the ice samples, which are 0.56 MPa for -10 °C ice, 0.69 MPa for -30 °C ice. A Hopkinson pressure bar was modified to launch ice balls which then impacted onto a rigid target of a four-meter-long aluminium bar. Strain gauges were used to record the force versus time history during the impact, together with high speed photography. Dimensional analyses have been successfully applied for the experimental data and empirical relationships have been obtained for prediction of the peak force and time corresponding to the peak force.

The results show that the force history in ice impact is significantly influenced by the size and impact velocity of ice balls. With the increase of size and impact velocity, both the peak force and time corresponding to the peak force increase. The temperature of ice balls also plays an important role in the impact by changing the tensile strength. Lower temperature results in higher peak force due to higher value of tensile strength. Time corresponding to the peak force is relatively insensitive to the temperature for velocities lower than 40 m/s; but for higher velocities, low temperature results in smaller time corresponding to the peak force.

Two empirical equations have been developed for the dimensionless peak force and the dimensionless time corresponding to the peak force in terms of dimensionless impact velocity, respectively, by using a power law relationship. The established equations are able to predict the peak force and time corresponding to the peak force in ice impact for a wide range of parameters studied. The measured impulse is approximately equal to the momentum input from the ice ball. The findings of the present study for these important quantities will offer great guidance in future investigations into structural responses subject to ice impact.

CRediT author statement

Siyu Chen: Investigation; Data Curation; Formal analysis; Writing – Original Draft; Writing – Review & Editing

Emad Gad: Conceptualization; Investigation; Supervision; Funding acquisition

Lihai Zhang: Conceptualization; Writing – Review & Editing; Project administration; Funding acquisition

Nelson Lam: Conceptualization; Writing – Review & Editing; Funding acquisition

Shanqing Xu: Investigation; Writing – Review & Editing

Guoxing Lu: Conceptualization; Methodology; Formal analysis; Writing – Review & Editing; Supervision; Funding acquisition

Declaration of interests

The authors declare that they have no known competing financial interests or personal relationships that could have appeared to influence the work reported in this paper.

Acknowledgements

This study is financially supported by the Australian Research Council through Linkage Project (ARC LP190100208). The authors are grateful to Mr Ian Bennie (General Manager of Ian Bennie and Associates)and to Mr Suresh Sutrave (Director of Atlite Skylights) for their valuable contributions as Partner Investigators of the Linkage project. The first author, Siyu Chen, wishes to thank Ms Chuxuan Shi and Mr Jintao Chu for their kind help in the preparation of the ice ball specimens. Guoxing Lu is grateful to Professor CR Calladine for the valuable comments on the work presented.

References

[1] Combescure, A., Chuzel-Marmot, Y. and Fabis, J., 2011. Experimental study of high-velocity impact and fracture of ice. *International Journal of Solids and Structures*, *48*(20), pp.2779-2790.

[2] Anghileri, M., Castelletti, L.M., Invernizzi, F. and Mascheroni, M., 2005. A survey of numerical models for hail impact analysis using explicit finite element codes. *International Journal of Impact Engineering*, *31*(8), pp.929-944.

[3] Cai, W., Zhu, L. and Qian, X., 2022. Dynamic responses of steel plates under repeated ice impacts. *International Journal of Impact Engineering*, *162*, pp.104129.

[4] Cai, W., Zhu, L., Yu, T.X. and Li, Y., 2020. Numerical simulations for plates under ice impact based on a concrete constitutive ice model. *International Journal of Impact Engineering*, *143*, pp.103594.

[5] Rhymer, J., Kim, H. and Roach, D., 2012. The damage resistance of quasi-isotropic carbon/epoxy composite tape laminates impacted by high velocity ice. *Composites Part A: Applied Science and Manufacturing*, *43*(7), pp.1134-1144.

[6] Park, H. and Kim, H., 2010. Damage resistance of single lap adhesive composite joints by transverse ice impact. *International Journal of Impact Engineering*, *37*(2), pp.177-184.

[7] Dolati, S., Fereidoon, A. and Sabet, A.R., 2014. Experimental investigation into glass fiber/epoxy composite laminates subjected to single and repeated high-velocity impacts of ice. *Iranian Polymer Journal*, *23*(6), pp.477-486.

[8] Kim, H., Welch, D.A. and Kedward, K.T., 2003. Experimental investigation of high velocity ice impacts on woven carbon/epoxy composite panels. *Composites Part A: Applied Science and Manufacturing*, *34*(1), pp.25-41.

[9] Tang, Z., Hang, C., Suo, T., Wang, Y., Dai, L., Zhang, Y. and Li, Y., 2017. Numerical and experimental investigation on hail impact on composite panels. *International Journal of Impact Engineering*, *105*, pp.102-108.

[10] Appleby-Thomas, G.J., Hazell, P.J. and Dahini, G., 2011. On the response of two commercially-important CFRP structures to multiple ice impacts. *Composite Structures*, *93*(10), pp.2619-2627.

[11] Wu, X., Li, Y., Cai, W., Guo, K. and Zhu, L., 2022. Dynamic responses and energy absorption of sandwich panel with aluminium honeycomb core under ice wedge impact. *International Journal of Impact Engineering*, *162*, pp.104137.

[12] Hammetter, C.I., Jones, R.L., Stauffacher, H.L. and Schoenherr, T.F., 2017. Measurement and modeling of supersonic hailstone impacts. *International Journal of Impact Engineering*, *99*, pp.48-57.

[13] Sun, J., Lam, N., Zhang, L., Ruan, D. and Gad, E., 2015. Contact forces generated by hailstone impact. *International Journal of Impact Engineering*, *84*, pp.145-158.

[14] Tan, X., Feng, X., Hu, Y., Xie, R., Yang, S., and Bai, Y., 2020. Experimental investigation on characteristics of layered ice spheres under high-velocity impact. *Explosion and Shock (in Chinese)*, *40*(11), pp.139-148.

[15] Tippmann, J.D., Kim, H. and Rhymer, J.D., 2013. Experimentally validated strain rate dependent material model for spherical ice impact simulation. *International Journal of Impact Engineering*, *57*, pp.43-54.

[16] Pereira, J.M., Padula, S.A., Revilock, D.M. and Melis, M.E., 2006. Forces generated by high velocity impact of ice on a rigid structure (No. NASA/TM-2006-214263).

[17] Singh, S., Masiulaniec, K., DeWitt, K. and Britton, R., 1994. Measurements of the impact forces of shed ice striking a surface. In *32nd Aerospace Sciences Meeting and Exhibit*, pp. 713.

[18] Kim, H. and Kedward, K.T., 2000. Modeling hail ice impacts and predicting impact damage initiation in composite structures. *AIAA Journal*, *38*(7), pp.1278-1288.

[19] Carney, K.S., Benson, D.J., DuBois, P. and Lee, R., 2006. A phenomenological high strain rate model with failure for ice. *International Journal of Solids and Structures*, *43*(25-26), pp.7820-7839.

[20] Pernas-Sánchez, J., Artero-Guerrero, J.A., Varas, D. and López-Puente, J., 2015. Analysis of ice impact process at high velocity. *Experimental Mechanics*, *55*(9), pp.1669-1679.

[21] Byers, H.R. and Braham, R.R., 1949. *The thunderstorm: report of the Thunderstorm Project*. US Government Printing Office.

[22] Haynes, F.D., 1978. *Effect of temperature on the strength of snow-ice* (Vol. 78, No. 27). U.S. Army Cold Regions Research and Engineering Laboratory, Hanover, New Hampshire.

[23] Schulson, E.M., 2001. Brittle failure of ice. *Engineering Fracture Mechanics*, *68*(17-18), pp.1839-1887.

[24] Hawkes, I. and Mellor, M., 1972. Deformation and fracture of ice under uniaxial stress. *Journal of Glaciology*, *11*(61), pp.103-131.

[25] Mellor, M. and Hawkes, I., 1971. Measurement of tensile strength by diametral compression of discs and annuli. *Engineering Geology*, *5*(3), pp.173-225.

[26] Currier, J.H. and Schulson, E.M., 1982. The tensile strength of ice as a function of grain size. *Acta Metallurgica*, *30*(8), pp.1511-1514.

[27] Gold, L.W., 1977. Engineering properties of fresh-water ice. *Journal of Glaciology*, *19*(81), pp.197-212.

[28] Li, D. and Wong, L.N.Y., 2013. The Brazilian disc test for rock mechanics applications: review and new insights. *Rock Mechanics and Rock Engineering*, *46*(2), pp.269-287.

[29] ASTM, 2016. D3967-16: Standard Test Method for Splitting Tensile Strength of Intact Rock Core Specimens, ASTM International, West Conshohocken, PA.

[30] Litwin, K.L., Zygielbaum, B.R., Polito, P.J., Sklar, L.S. and Collins, G.C., 2012. Influence of temperature, composition, and grain size on the tensile failure of water ice: Implications for erosion on Titan. *Journal of Geophysical Research: Planets*, *117*(E8).

[31] Buckingham, E., 1914. On physically similar systems; illustrations of the use of dimensional equations. *Physical Review*, *4*(4), pp.345.

[32] Johnson, K.L., 1987. *Contact Mechanics*. Cambridge university press.

[33] Perera, S., Lam, N., Pathirana, M., Zhang, L., Ruan, D. and Gad, E., 2016. Deterministic solutions for contact force generated by impact of windborne debris. *International Journal of Impact Engineering*, *91*, pp.126-141.

[34] Yang, Y., Lam, N.T.K. and Zhang, L., 2012. Estimation of response of plate structure subject to low velocity impact by a solid object. *International Journal of Structural Stability and Dynamics*, *12*(06), pp.1250053.

[35] Yang, Y., Lam, N.T.K. and Zhang, L., 2012. Evaluation of simplified methods of estimating beam responses to impact. *International Journal of Structural Stability and Dynamics*, *12*(03), pp.1250016.

[36] Petrovic, J. J., 2003. Review of mechanical properties of ice and snow. *Journal of Materials Science*, *38*(1), pp. 1-6.